



Lab Resource: Genetically-Modified Multiple Cell Lines

## Generation of heterozygous (MCRIi030-A-1) and homozygous (MCRIi030-A-2) *NR2F2*/COUP-TFII knockout human iPSC lines

Lucas G.A. Ferreira<sup>a,b</sup>, Mauricio C. Cabral-da-Silva<sup>b,c,d</sup>, Svenja Pachernegg<sup>b,c</sup>,  
Jocelyn A. van den Bergen<sup>b</sup>, Gorjana Robevska<sup>b</sup>, Katerina Vlahos<sup>b</sup>, Sara E. Howden<sup>b,d</sup>,  
Elizabeth S. Ng<sup>b,c,d</sup>, Magnus R. Dias-da-Silva<sup>a</sup>, Andrew H. Sinclair<sup>b,c</sup>, Katie L. Ayers<sup>b,c,\*</sup>

<sup>a</sup> Laboratory of Molecular and Translational Endocrinology (LEMT), Endocrinology Division, Department of Medicine, Escola Paulista de Medicina, Universidade Federal de São Paulo, São Paulo, Brazil

<sup>b</sup> The Murdoch Children's Research Institute, Melbourne, Australia

<sup>c</sup> Department of Paediatrics, The University of Melbourne, Melbourne, Australia

<sup>d</sup> Novo Nordisk Foundation Center for Stem Cell Medicine (reNEW), Murdoch Children's Research Institute, Melbourne, Australia

### A B S T R A C T

The *NR2F2* gene encodes the transcription factor COUP-TFII, which is upregulated in embryonic mesoderm. Heterozygous variants in *NR2F2* cause a spectrum of congenital anomalies including cardiac and gonadal phenotypes. We generated heterozygous (MCRIi030-A-1) and homozygous (MCRIi030-A-2) *NR2F2*-knockout induced pluripotent stem cell (iPSC) lines from human fibroblasts using a one-step protocol for CRISPR/Cas9 gene-editing and episomal-based reprogramming. Both iPSC lines exhibited a normal karyotype, typical pluripotent cell morphology, pluripotency marker expression, and the capacity to differentiate into the three embryonic germ layers. These lines will allow us to explore the role of *NR2F2* during development and disease.

### 1. Resource Table

(continued)

Unique stem cell line identifier	Cell line 1: MCRIi030-A-1 Cell line 2: MCRIi030-A-2		MCRIi030-A-2: Compound heterozygous mutations: deletion of <i>NR2F2</i> exons 2–3 and frameshift in the <i>NR2F2</i> exon 2
Alternative name(s) of stem cell line	Cell line 1: 522/NR2F2-KO_het Cell line 2: 522/NR2F2-KO_hom	Associated disease	N/A
Institution	The Murdoch Children's Research Institute	Gene/locus	<i>NR2F2</i> gene/15q26.2
Contact information of the reported cell line distributor	A/Prof Katie Ayers <a href="mailto:katie.ayers@mcri.edu.au">katie.ayers@mcri.edu.au</a>	Method of modification/user-customisable nuclease (UCN) used, the resource used for design optimisation	CRISPR/Cas9
Type of cell line	iPSC	User-customisable nuclease (UCN) delivery method	Encoding plasmid transfection
Origin	Human	All double-stranded DNA genetic material molecules introduced into the cells	Reprogramming and gene-editing plasmids
Additional origin info (applicable for human ESC or iPSC)	Age: 16 FW Sex: Female Ethnicity: N/A	Analysis of the nuclease-targeted allele status	PCR and Sanger sequencing
Cell Source	Fibroblasts	Method of the off-target nuclease activity prediction and surveillance	Top off-target site analyzed by PCR/sequencing in genomic exons
Method of reprogramming	Episomal	Descriptive name of the transgene	N/A
Clonality	Clonal, manually isolated	Eukaryotic selective agent resistance cassettes (including inducible, gene/cell type-specific)	N/A
Evidence of the reprogramming transgene loss (including genomic copy if applicable)	PCR	Inducible/constitutive expression system details	N/A
The cell culture system used	E7 + 100 $\mu$ M sodium butyrate and E8		
Type of the Genetic Modification	Induced mutation: MCRIi030-A-1: Heterozygous deletion of <i>NR2F2</i> exons 2–3		

(continued on next column)

(continued on next page)

\* Corresponding author at: The Murdoch Children's Research Institute, Melbourne, Australia.

E-mail address: [katie.ayers@mcri.edu.au](mailto:katie.ayers@mcri.edu.au) (K.L. Ayers).

(continued)

Date archived/stock creation date	December 9, 2023
Cell line repository/bank	Cell line 1: <a href="https://hpscreg.eu/cell-line/MCRIi030-A-1">https://hpscreg.eu/cell-line/MCRIi030-A-1</a> Cell line 2: <a href="https://hpscreg.eu/cell-line/MCRIi030-A-2">https://hpscreg.eu/cell-line/MCRIi030-A-2</a>
Ethical/GMO work approvals	Cell source was acquired from Coriell Institute for Medical Research <a href="https://www.coriell.org/">https://www.coriell.org/</a>
Addgene/public access repository recombinant DNA sources' disclaimers (if applicable)	Addgene #80427, #80424, #20927, #20922, #20923, and #98748

2. Resource utility

Heterozygous loss-of-function variants in *NR2F2* have been associated with a broad spectrum of congenital anomalies (Polvani et al., 2019; Ganapathi et al., 2023). The heterozygous and homozygous *NR2F2*-knockout iPS cells MCRIi030-A-1 and MCRIi030-A-2 generated here provide a cell model to explore the role of *NR2F2* during development and the mechanisms of *NR2F2* haploinsufficiency in human pathologies with developmental origins.

3. Resource details

The nuclear receptor subfamily 2 group F member 2 (*NR2F2*) gene encodes the transcription factor chicken ovalbumin upstream promoter transcription factor 2 (COUP-TFII). COUP-TFII is an orphan nuclear receptor due to a lack of known natural ligands (Polvani et al., 2019). The canonical COUP-TFII protein presents an N-terminal activation binding motif (1-78aa) and a DNA-binding domain (79-151aa) encoded by exon 1, a hinge region (152-176aa) and a C-terminal ligand-binding domain (177-411aa) encoded by exons 2 and 3 (Polvani et al., 2019). Two other COUP-TFII isoforms are expressed from *NR2F2* gene lacking the DNA-binding domain due to independent transcription start sites selecting alternative exon 1 (Polvani et al., 2019). *NR2F2*/COUP-TFII expression is upregulated in the embryonic mesoderm and heterozygous variants in this gene cause a spectrum of malformations, including congenital heart disease (CHD), congenital diaphragmatic hernia (CDH) and 46,XX ovotesticular differences of sex development (DSD) (Bashamboo et al., 2018; Carvalheira et al., 2019; Ganapathi et al., 2023).

We generated heterozygous (MCRIi030-A-1) and homozygous (MCRIi030-A-2) *NR2F2*-knockout iPS cell lines from human fibroblasts using CRISPR/Cas9 technology and episomal-based reprogramming system, which forced expression of miR302/367 cluster, OCT3/4, SOX2, NANOG, c-MYC, KLF4, LIN28, and SV40 large T antigen (SV40LT). SV40LT was included to counteract any toxic effects of c-MYC expression, which was added to improve the reprogramming efficiency. We used a single guide RNA (sgRNA) specific to *NR2F2* exon 2, which is a shared exon among *NR2F2*/COUP-TFII isoforms, and a sgRNA to the 3'UTR of *NR2F2* (Fig. 1A). Sequencing revealed introduction of a heterozygous deletion of exons 2–3 between Cas9 target sites (MCRIi030-A-1), and compound heterozygous alleles in the second line; a deletion of exons 2–3 and 7 bp deletion at Cas9 target site 1, which causes a frameshift and premature stop codon (p.Gly160fs\*5, MCRIi030-A-2) (Fig. 1B). Both lines formed colonies comprising tightly packed cells with large nucleus-to-cytoplasm ratio and prominent nucleoli (Fig. 1C). The pluripotency marker SOX2 was abundantly detected by immunofluorescence staining (Fig. 1D). Using flow cytometry, we observed that over 89% of viable cells expressed the pluripotency markers TRA-1-60, TRA-1-81, SSEA-4, and OCT3/4 (Fig. 1E). Multiplexed PCR was performed to confirm loss of reprogramming plasmids after 10 passages (Supplementary Fig. S1B). Both cell lines had the ability to undergo parallel directed differentiation of embryoid bodies (EB) for the three germ layers (Supplementary Fig. S1D). Specifically, immunofluorescence studies identified the ectodermal marker MAP2, the mesodermal

marker SMA and the endodermal markers SOX17 and GATA4 (Fig. 1F). Array analysis demonstrated that the two cell lines have a normal female chromosome complement [arr(X,1–22)x2] with SNPduo comparative analysis showing an identical genotype to the parental cell line. Thus, no major perturbations in genomic integrity occurred during reprogramming and nuclease activity. Furthermore, both iPS cell lines were free of mycoplasma contamination (Supplementary Fig. S1A). No mutations were detected at the top predicted off-target sites in coding exons of the *TTN* and *LTBP1* genes (Supplementary Fig. S1C).

As *NR2F2*/COUP-TFII is not expressed in undifferentiated iPS cells, we used EBs differentiated into mesoderm to confirm that the induced genetic modifications in *NR2F2* gene led to premature termination of translation and loss of protein. Western blot analysis showed decreased COUP-TFII protein levels in mesodermal EBs derived from the MCRIi030-A-1 line compared to unmodified cells and complete absence of the protein in mesodermal EBs from the MCRIi030-A-2 line (Fig. 1G, Supplementary Fig. S1E). Characterisation and validation analyses are summarised in Table 1.

4. Materials and methods

4.1. iPS cell generation and gene editing

sgRNAs (Table 2) were designed with CRISPOR (<http://crispor.tefor.net>) and cloned into pSMART-sgRNA plasmids. We used a one-step protocol for generation of clonally derived gene-edited iPS cell lines from healthy human fibroblasts (Coriell Institute ID: GM04522) as previously described (Howden et al., 2018). Gene-editing and reprogramming factors were introduced into fibroblasts using the Neon Transfection System (1400 V, 20 ms, 2 pulses). Transfected cells were plated on Matrigel (Corning) coated plates in fibroblast medium (DMEM + 15 % FBS). Medium was switched to E7 + butyrate after 3 days and changed every other day until first iPS cell colonies appeared. Media was then switched to Essential 8 (E8) medium (ThermoFisher Scientific) and individual iPS cell colonies were picked and expanded. Cells were kept at 5 % CO<sub>2</sub>, 20 % O<sub>2</sub> and 37 °C with daily medium changes. Cells were passaged at a ratio of 1:3–1:6 every 3–4 days using 0.5 mM EDTA/PBS.

4.2. Genotyping and sequencing

DNA was extracted using DNeasy Blood & Tissue Kit (Qiagen) according to the instructions. PCR was performed using GoTaq®DNA Polymerase (Promega) with primers flanking Cas9 target sites and binding within the intervening sequence between Cas9 target sites (Table 2). Products were visualized by gel electrophoresis and purified using ExoSAP-IT™ (ThermoFisher Scientific). Sanger sequencing was performed with BigDye™ Terminator v3.1 Cycle Sequencing Kit (ThermoFisher Scientific) by AGRF (Melbourne, Australia).

4.3. Immunofluorescence

Cells were fixed with 4% Paraformaldehyde for 15 min at room temperature, permeabilized in 1% Triton X-100 (Sigma) for 10 min and blocked in 2% BSA (Sigma) for 60 min. Cells were incubated with primary antibodies at 4 °C overnight, followed by secondary antibodies for 2 h at room temperature (Table 2). Nuclei were stained with DAPI and images were captured with an LSM780 confocal microscope (Zeiss).

4.4. Flow cytometry

Dissociated iPS cells at passage 12 were incubated with directly conjugated antibodies for 30 min on ice (Table 2). Cells were fixed/permeabilized prior to intracellular OCT3/4 staining using eBioscience Transcription Factor Staining Buffer Set (ThermoFisher Scientific). Samples were analysed using an LSR Fortessa (BD Bioscience).

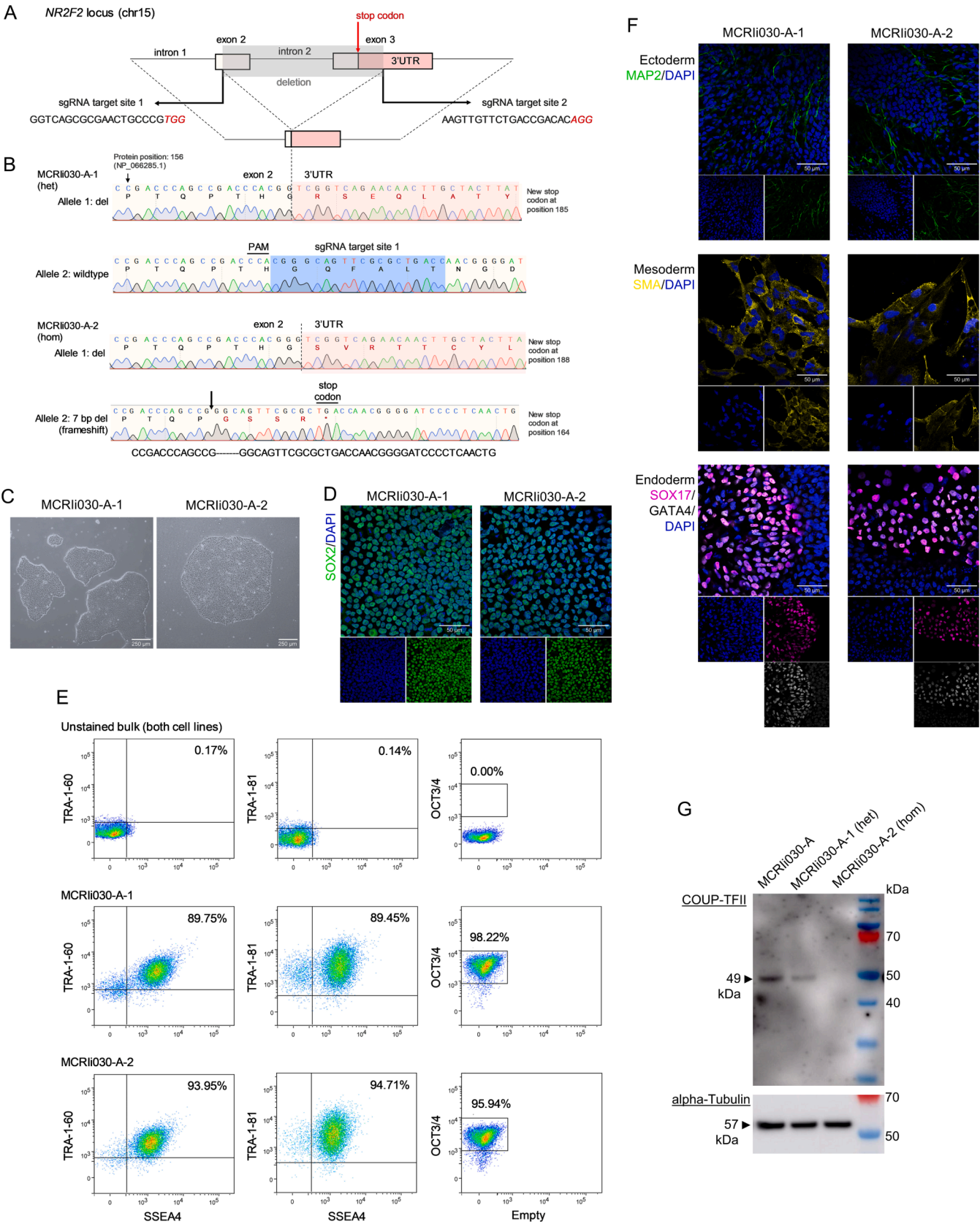


Fig. 1. Generation and validation of the heterozygous (MCRli030-A-1) and homozygous (MCRli030-A-2) *NR2F2* knockout iPSC lines.

**Table 1**  
Characterization and validation.

Classification	Test	Result	Data
Morphology	Photography brightfield	Normal morphology	Fig. 1C
Pluripotency status evidence for the described cell line	Qualitative analysis (immunofluorescence)	SOX2	Fig. 1D
	Quantitative analysis (Flow cytometry)	MCRi030-A-1 and MCRi030-A-2: OCT3/4: 98.22% and 95.94%; TRA-1-60 + SSEA4: 89.75% and 93.95%; TRA-1-81 + SSEA4: 89.45% and 94.71%.	Fig. 1E
Karyotype	Karyotype (SNP array) and resolution	MCRi030-A-1: arr(X,1–22)x2 MCRi030-A-2: arr(X,1–22)x2 Resolution 0.50 Mb	Fig. S1A
Genotyping for the desired genomic alteration/allelic status of the gene of interest	PCR across the edited site/Sanger sequencing	MCRi030-A-1: heterozygous deletion; MCRi030-A-2: compound heterozygous mutations (deletion and frameshift)	Fig. 1B
	Evaluation of the - (homo-/hetero-/hemi-) zygous status of introduced genomic alteration(s)	As mentioned above	Fig. 1B
	Transgene-specific PCR (when applicable)	N/A	N/A
Verification of the absence of random plasmid integration events	PCR/Southern	PCR showed loss of reprogramming plasmids (after 10 passages)	Fig. S1B
Parental and modified cell line genetic identity evidence	STR analysis, microsatellite PCR (mPCR) or specific (mutant) allele seq	SNPduo comparative analysis performed to compare parental and both derived clones	Supplementary file, submitted in the archive with journal
Mutagenesis/genetic modification outcome analysis	Sequencing (genomic DNA PCR)	Sanger sequencing confirmed a heterozygous deletion of <i>NR2F2</i> exons 2–3 (MCRi030-A-1) and compound heterozygous mutations (deletion of <i>NR2F2</i> exons 2–3 and frameshift in the <i>NR2F2</i> exon 2) (MCRi030-A-2)	Fig. 1B
	PCR-based analyses Western blotting (for knock-outs, KOs)	As mentioned above Western blot showed that COUP-TFII is detected in lower intensity in MCRi030-A-1 compared to control cell line and not detected in MCRi030-A-2	Fig. 1B Fig. 1G, Fig. S1E
Off-target nuclease activity analysis	PCR/Sanger sequencing across the predicted top likely off-target site spanning coding exons	Lack of NHEJ-caused mutagenesis in the top predicted off-target Cas nuclease activity (in coding exons)	Fig. S1C
Specific pathogen-free status	Mycoplasma	Mycoplasma testing by RT-PCR. Negative	Fig. S1A
Multilineage differentiation potential	e.g. Embryoid body formation (immunofluorescence)	Positive for: Ectoderm: MAP2 Endoderm: SOX17 and GATA4 Mesoderm: A-SMA	Fig. 1F, Fig. S1D
Donor screening	HIV 1 + 2 Hepatitis B, Hepatitis C	N/A	N/A
Genotype - additional histocompatibility info	Blood group genotyping	N/A	N/A
	HLA tissue typing	N/A	N/A

#### 4.5. Embryoid body formation

iPSCs at passage 14 were incubated with 1  $\mu$ M Thiazovivin (Selleck Chemicals) 3 h prior to dissociation with 0.5 mM EDTA/PBS. iPSCs were transferred to 60  $\times$  15 mm culture dishes on EB maintenance medium (DMEM/F12, 4 ng/mL bFGF, 0.1% PVA, ITSE, and nonessential aminoacids) supplemented with 1  $\mu$ M Thiazovivin for 24 h and kept in swirling suspension culture (60 rpm). From day 0, cells were incubated with 3  $\mu$ M CHIR + 2  $\mu$ M SB431542, 25 ng/mL BMP4, and 50 ng/mL Activin-A for differentiation into ectodermal, mesodermal e endodermal EBs, respectively. Medium supplementation for ectodermal EBs was replaced for 300 nM retinoic acid, 0.25x B27, and 0.5x N2 from day 3

onwards. On day 6, EBs were plated on coverslips for 4 days.

#### 4.6. Western blot

Cell lysates of mesodermal EBs at day 5 were prepared with RIPA buffer containing protease inhibitor (Roche, 05892970001). 2  $\mu$ g of denatured protein lysates were run on SDS-PAGE conditions and transferred to PVDF membrane. Blots were performed using standard protocols (antibodies listed in Table 2).



**Table 2**  
Reagents details.

Antibodies and stains used for immunocytochemistry/flow-cytometry			
	Antibody	Dilution	Company Cat # and RRID
Pluripotency Markers	Rabbit anti-SOX2	1:300	Abcam Cat# ab97959, RRID: AB_2341193;
	PE anti-OCT3/4	1:100	Thermo Fisher Scientific Cat# 12–5841–80, RRID: AB_914364;
	BV421 anti-TRA-1–60	1:100	BD Biosciences Cat# 562,711, RRID: AB_2737738;
	PE/Cy7 anti-SSEA-4	1:100	BioLegend Cat# 330,420, RRID: AB_2629631;
	Alexa Fluor 647 anti-TRA-1–81	1:100	BioLegend Cat# 330,706, RRID: AB_1089242
Differentiation Markers	Mouse anti-Actin, a-Smooth Muscle	1:25	Sigma-Aldrich Cat# A5228, RRID: AB_262054
	Chicken anti-MAP2	1:5000	Abcam Cat# ab5392, RRID: AB_2138153
	Rabbit anti-SOX17	1:100	Abcam Cat# ab224637, RRID: AB_2801385
	Mouse anti-GATA4	1:400	Santa Cruz Cat# sc-25310, RRID: AB_627667
Western blot primary antibodies	Mouse anti-NR2F2	1:1000	Abcam Cat# ab41859, RRID: AB_742211
	Mouse anti-alpha Tubulin HRP	1:5000	Abcam Cat# ab40742, RRID: AB_880625
Secondary antibodies	Donkey anti-Rabbit IgG (H + L) Highly Cross-Adsorbed Secondary Antibody, Alexa Fluor™ 488	1:1000	Thermo Fisher Scientific Cat# A21206, RRID: AB_2535792;
	Donkey anti-Mouse IgG (H + L) Highly Cross-Adsorbed Secondary Antibody, Alexa Fluor™ 594	1:1000	Thermo Fisher Scientific Cat# A21203, RRID: AB_141633
	Goat anti-Chicken IgY (H + L) Secondary Antibody, Alexa Fluor™ 488	1:1000	Thermo Fisher Scientific Cat# A11039, RRID: AB_2534096
	Rabbit anti-mouse HRP	1:10000	Agilent Cat# P0260, RRID: AB_2636929
Nuclear stain	DAPI	0.125 µg/mL	Thermo Fisher Scientific Cat# D1306, RRID: AB_2629482
Site-specific nuclease			
Nuclease information	SpCas9-Gem	Howden et al. Stem Cell Reports 2016 Sep; 7(3):508–17	
Delivery method	Electroporation	Neon Transfection System (1400 V, 20 ms, 2 pulses)	
Selection/enrichment strategy	Clones manually isolated		
Primers and Oligonucleotides used in this study			
	Target	Forward/Reverse primer (5´-3´)	

**Table 2 (continued)**

Antibodies and stains used for immunocytochemistry/flow-cytometry			
	Antibody	Dilution	Company Cat # and RRID
Genotyping by PCR	NR2F2 across deletion	GAGGCTGGTCATTAAGTGTGG/CTCCCAATCTCCTTAAATGC	
	NR2F2 protospacer 1	GAGGCTGGTCATTAAGTGTGG/CGCAAATGTTCTCGATACCC	
	NR2F2 within deletion	ACTTGGGCTGGATATGGATG/TGGGTGACTAGGTTCCAAGC	
	NR2F2 protospacer 2	CCCATCGAAACCTCATCC/CTCCCAATCTCCTTAAATGC	
Targeted mutation analysis/sequencing	NR2F2 protospacer 1 and amplicon across deltion	GGTCATTAAGTGTGGAGTGTG	
	NR2F2 protospacer 2	GGGATATGTTACTGTCCG	
Potential random integration-detecting PCRs	Reprogramming plasmids: origin of replication (OriP) ampicillin resistance (ampR) gene	AGCTACCGATAAGCGGACC/CCCTCGTGAATCCTGACC CAGTCTATTAATTGTTGCCGGG/ GCTATGTGGCGCGGTATTAT	
gRNA oligonucleotide/crRNA sequence	NR2F2 gene specific	sgRNA 1: GGTCAGCGCGAACTGCCCG sgRNA 2: AAGTTGTTCTGACCGACAC	
Oligo for cloning sgRNA	NR2F2 guide primers 1 and 2	sgRNA 1: CACCGGGTCAGCGCGAACTGCCCG/ AAACCGGCAGTTCGCGCTGACCC sgRNA 2: CACCGAAGTTGTTCTGACCGACAC/ AAACGTGTGCGTCAGAACAACTTC	
Genomic target sequence(s)	sgRNA 1: NR2F2 exon 2 sgRNA 2: 3'UTR of NR2F2	Homo sapiens chromosome 15, GRCh38.p14: sgRNA 1 target site: 96334113–96334135 sgRNA 2 target site: 96337839–96337861	
Bioinformatic gRNA on- and off-target binding prediction tool used, specific sequence/ outputs link(s)	CRISPOR	sgRNA 1: <a href="http://crispor.tefor.net/crispor.py?batchId=gDkMQr2zXBh045t3iW2f">http://crispor.tefor.net/crispor.py?batchId=gDkMQr2zXBh045t3iW2f</a> sgRNA 2: <a href="http://crispor.tefor.net/crispor.py?batchId=o8GQD0udVQqXiaV0x3W">http://crispor.tefor.net/crispor.py?batchId=o8GQD0udVQqXiaV0x3W</a>	
Primers for top off-target mutagenesis predicted site sequencing (for CRISPR/Cas9)	OT sgRNA 1: TTN exon 295 (chr 2)	OT sgRNA 1: Homo sapiens chromosome 2, GRCh38.p14: 237841–238213 GGCATTGGAGAACCTGGAGA/CTCCGGCTTCATTTTGGCA	
	OT sgRNA 2: LTBP1 exon 33 (chr 2)	OT sgRNA 2: Homo sapiens chromosome 2, GRCh38.p14: 33443254–33443460 TCTGCCCTTTCTCTTCCAGG/TGAGATACGGGGTGTCCAGGA	

4.7. Mycoplasma detection

Absence of mycoplasma contamination was confirmed by PCR by the commercial service provider Cerberus Sciences (Adelaide, Australia).

#### 4.8. Karyotyping

Molecular karyotypes were analysed using the Illumina Infinium GSA-24 v3.0 array using human reference sequence GRCh38/hg38 (Dec 2013). The SNP array was compared to corresponding iPSC line using SNPduo comparative analysis (<https://pevsnerlab.kennedykrieger.org/SNPduo/>).

#### 4.9. Off-target analysis

Potential off-targets of Cas9 activity were determined using CRISPOR and assessed by PCR/Sanger sequencing.

#### CRedit authorship contribution statement

**Lucas G.A. Ferreira:** Writing – original draft, Visualization, Validation, Methodology, Investigation, Formal analysis, Data curation. **Mauricio C. Cabral-da-Silva:** Validation, Methodology, Investigation. **Svenja Pachernegg:** Supervision, Funding acquisition, Conceptualization. **Jocelyn A. van den Bergen:** Methodology, Investigation, Conceptualization. **Gorjana Robevska:** Methodology, Investigation. **Katerina Vlahos:** Visualization, Validation, Supervision, Resources, Methodology, Investigation, Formal analysis, Data curation, Conceptualization. **Sara E. Howden:** Resources, Methodology, Formal analysis, Conceptualization. **Elizabeth S. Ng:** Resources, Methodology, Investigation. **Magnus R. Dias-da-Silva:** Supervision, Resources, Funding acquisition. **Andrew H. Sinclair:** Supervision, Resources, Project administration, Funding acquisition. **Katie L. Ayers:** Visualization, Supervision, Resources, Investigation, Funding acquisition, Formal analysis, Conceptualization.

#### Declaration of competing interest

The authors declare that they have no known competing financial

interests or personal relationships that could have appeared to influence the work reported in this paper.

#### Appendix A. Supplementary data

Supplementary data to this article can be found online at <https://doi.org/10.1016/j.scr.2024.103374>.

#### References

- Bashamboo, A., Eozenou, C., Jorgensen, A., Bignon-Topalovic, J., Siffroi, J.P., Hyon, C., Tar, A., Nagy, P., Solyom, J., Halász, Z., Paye-Jaouen, A., Lambert, S., Rodriguez-Burítica, D., Bertalan, R., Martinerie, L., Rajpert-De Meyts, E., Achermann, J.C., McElreavey, K., 2018. Loss of function of the nuclear receptor NR2F2, encoding COUP-TF2, causes testis development and cardiac defects in 46, XX children. *Am. J. Hum. Genet.* 102 (3), 487–493. <https://doi.org/10.1016/j.ajhg.2018.01.021>. Epub 2018 Feb 22. PMID: 29478779; PMCID: PMC5985285.
- Carvalho, G., Malinverni, A.M., Moyses-Oliveira, M., Ueta, R., Cardili, L., Monteagudo, P., Mathez, A.L.G., Verreschi, I.T., Maluf, M.A., Shida, M.E.F., Leite, M.T.C., Mazzotti, D., Melaragno, M.I., Dias-da-Silva, M.R., 2019. The natural history of a man with ovotesticular 46,XX DSD caused by a novel 3-Mb 15q26.2 deletion containing NR2F2 gene. *J. Endocr. Soc.* 3 (11), 2107–2113. <https://doi.org/10.1210/js.2019-00241>. Erratum in: *J. Endocr. Soc.* 2020 Mar 10;4(3):bvaa022. PMID: 31687637; PMCID: PMC6821239.
- Ganapathi, M., Matsuoka, L.S., March, M., Li, D., Brokamp, E., Benito-Sanz, S., White, S.M., Lachlan, K., Ahimaz, P., Sewda, A., Bastarache, L., Thomas-Wilson, A., Stoler, J.M., Bramswig, N.C., Baptista, J., Stals, K., Demurger, F., Cogne, B., Isidor, B., Bedeschi, M.F., Peron, A., Amiel, J., Zackai, E., Schacht, J.P., Iglesias, A.D., Morton, J., Schmetz, A., Undiagnosed Diseases Network, Seidel, V., Lucia, S., Baskin, S.M., Thiffault, I., Cogan, J.D., Gordon, C.T., Chung, W.K., Bowdin, S., Bhoj, E., 2023. Heterozygous rare variants in NR2F2 cause a recognizable multiple congenital anomaly syndrome with developmental delays. *Eur. J. Hum. Genet.* 31 (10), 1117–1124. <https://doi.org/10.1038/s41431-023-01434-5>. Epub 2023 Jul 27. PMID: 37500725; PMCID: PMC10545729.
- Howden, S.E., Thomson, J.A., Little, M.H., 2018. Simultaneous reprogramming and gene editing of human fibroblasts. *Nat. Protoc.* 13 (5), 875–898. <https://doi.org/10.1038/nprot.2018.007>. Epub 2018 Apr 5. PMID: 29622803; PMCID: PMC5997775.
- Polvani, S., Pepe, S., Milani, S., Galli, A., 2019. COUP-TFII in health and disease. *Cells* 9 (1), 101. <https://doi.org/10.3390/cells9010101>. PMID: 31906104; PMCID: PMC7016888.